

THE EFFECTS OF ANTENNA DIRECTIVITY ON PATH LOSS AND MULTIPATH PROPAGATION IN UWB INDOOR WIRELESS CHANNELS

Jason A. Dabin, *Student Member, IEEE*, Nan Ni, Alexander M. Haimovich, *Senior Member, IEEE*, Edip Niver, *Member, IEEE*, Haim Grebel, *Senior Member, IEEE* {grebel@njit.edu}

New Jersey Institute of Technology
University Heights, Newark, NJ 07102

Abstract— The effects of antenna directivity on path loss and multipath propagation in the ultra-wideband (UWB) indoor channel are analyzed for different transmitter/receiver (Tx/Rx) antenna combinations in the 2 GHz to 6 GHz frequency band. A statistical model of the path loss in the channel is presented, where the parameters in the model (i.e., path loss exponent and shadow fading statistics) are dependent on the particular Tx/Rx antenna combination. Time domain statistics of the channel (i.e., mean delay spread and RMS delay spread) are analyzed thoroughly for each antenna combination. There is a significant reduction in RMS delay spread when directional antennas are used at the transmitter and receiver as opposed to using omni-directional antennas. Results show that directional antennas can be used as an effective way of mitigating the effects of multipath propagation in UWB indoor channels.

I. INTRODUCTION

Ultra-wideband (UWB) technology is being considered as a wireless air interface for high-speed data transmission (e.g., wireless PAN IEEE standard 802.15.3a). For wideband systems, it is well known that multipath delay spread in the wireless channel limits data rates due to transmission errors caused by intersymbol interference (ISI). One method to mitigate the effects of multipath propagation is to use directional antennas. The radiation pattern or beamwidth of a directional antenna accepts only multipath signals that arrive within the beam pattern of the antenna, which therefore limits the amount of multipath received in the channel, resulting in less delay spread and the ability to achieve higher data rates. A UWB device defined by the Federal Communications Commission (FCC) must have a -10 dB fractional bandwidth greater than or equal to 20% of the center frequency or have a minimum bandwidth of 500 MHz [1]. To understand the UWB propagation channel (i.e., path loss and multipath characteristics), field measurements must be performed and analyzed thoroughly. UWB channels have been studied using both time and frequency domain channel sounding techniques in office and residential environments [2]-[5]. These measurements

did not include the effects of antenna directivity on the channel. Moreover, line of sight (LOS) measurements in classrooms and laboratories were not carried out extensively. This paper examines the effects of antenna directivity on path loss and multipath propagation in a college campus building at the New Jersey Institute of Technology (NJIT). A statistical model of the path loss in the UWB propagation channel for different omni-directional and directional antenna combinations is presented. Multipath characteristics of the channel are analyzed extensively using the first and second central moments of the measured impulse responses.

II. MEASUREMENT SYSTEM AND PROCEDURE

Frequency response measurements of the indoor UWB channel were performed using a frequency domain channel sounder configuration shown in Fig. 1. The channel was swept from 2 GHz to 6 GHz in intervals of 5 MHz, at a rate of 400 ms. The frequency response of the channel was measured using a Hewlett Packard 8510C Vector Network Analyzer (VNA). The VNA measures the magnitude and phase of each frequency component and therefore, the inverse discrete Fourier transform (IDFT) can be used to convert the frequency domain channel response into the time domain channel response for analysis in the temporal domain. Given the frequency spacing the time domain window can detect a multipath component arrival of up to 200 ns. This is a reasonable window length given that multipath arrivals have not been detected beyond 160 ns for transmitter/receiver (Tx/Rx) separation distances of less than 10 m [5]. Three Tx/Rx vertically polarized antenna combinations were tested using omni-directional and directional antennas. The omni-directional antenna is a linear polarized conical monopole antenna which is omni-directional in the azimuth plane with a typical gain of 0 dBi. The directional antenna is a linear polarized log periodic antenna with a half power beamwidth equal to 65° in the E-plane and a 100° in the H-plane and has an approximate gain of 5.6 dBi. Measurements were performed in a classroom and laboratory setting in the Faculty Hall building at NJIT.

All measurements were made while the transmitter and receiver antennas remained stationary and within line of sight of each other. The channel was kept stationary during measurements by ensuring there was no movement in the surrounding environment. The three Tx/Rx antenna combinations tested were: omni-directional/omni-directional, directional/directional, and omni-directional/directional antenna combinations, respectively. Measurements were made between 1 m and 10 m in intervals of 1 m with the exception of the classroom where measurements extended up to a maximum of 9 m. A total of seventy-eight locations were measured for each antenna combination with the exception of the omni-directional/directional case in which sixty-eight locations were measured. Ten snapshots of the channel frequency response were recorded per receiver location. The VNA was calibrated with respect to a 1 m reference distance inside an anechoic chamber for each antenna combination so that all measurements depend solely on the channel response. A back-to-back calibration was also carried out to assess the path loss in the channel at 1 m, which includes the antennas as well. The measured path loss at 1 m in the anechoic chamber and the pathloss computed by averaging over the same number of frequencies using the Friis free space equation in (1) resulted in a difference of at most 0.13 dB for all three antenna combinations. Therefore, a Tx/Rx separation distance of 1 m in the anechoic chamber was considered an adequate reference distance. The free space path loss is given by:

$$PL_{FS}(d) = \frac{G_{tx} G_{rx} \lambda^2}{(4\pi)^2 d^2}, \quad (1)$$

where $PL_{FS}(d)$ denotes the free space path loss, λ is the wavelength in meters, d is the distance in meters, and G_{tx} and G_{rx} denote the transmit and receive antenna gains, respectively. The Tx/Rx antennas were each set to a height of 1.4 m for all measurements.

III. LARGE SCALE FADING

The path loss of the channel represents the attenuation a signal undergoes when transmitted through the medium. The frequency response obtained from the VNA was referenced to 1 m as described in the measurement procedure. The average path loss of the channel is computed from:

$$PL(d) = \frac{1}{NK} \sum_{i=1}^N \sum_{j=1}^K |H(f_i, x_j; d)|^2, \quad (2)$$

where $H(f_i, x_j; d)$ is the frequency response of the channel, which represents the received power relative to the transmitted power per frequency component or,

rather the attenuation in the channel over the 2 GHz to 6 GHz frequency range. N represents the number of frequency components f measured in the channel. K represents the number of snapshots denoted by x , and d is the separation distance between the Tx/Rx antennas in meters.

It is well known that the mean path loss referenced to a distance d_0 can be modeled as a function of distance using equation (3) [2][6][7], where α is the path loss exponent and the path loss is represented as a positive quantity:

$$\overline{PL}(d; d_0) \propto \left(\frac{d}{d_0}\right)^\alpha. \quad (3)$$

By logarithmically transforming equation (3) and including the path loss at d_0 , the mean path loss in dB can be modeled linearly as a function of the logarithmic distance. The mean path loss model does not account for the clutter present in the environment at different locations with the same Tx/Rx separation distance. As the clutter in the environment changes from location to location, so does the received power, which introduces a random change in the path loss. This random variation has been shown to be log-normally distributed with zero mean [2][4], and is known as log-normal shadowing. Therefore, the path loss in the channel is log-normally distributed with a mean that linearly changes with distance and is modeled as:

$$PL_{dB}(d) = PL_{dB}(d_0) + 10 \cdot \alpha \log\left(\frac{d}{d_0}\right) + X, \quad (4)$$

where $PL_{dB}(d_0)$ denotes the mean path loss at 1 m, $10 \cdot \alpha \log(d/d_0)$ denotes the mean path loss referenced to 1 m, and X is a zero mean log-normal random variable in dB. The mean path loss at d_0 and the path loss exponent α (or rather, the slope of the mean of equation (4)) were determined through regression analysis using the method of least squares. That is, the path loss at d_0 and the slope α were taken as estimates for which the sum of the squares of the errors between the straight line and the measured data is a minimum. The difference between the least squares fit and the measured data is represented by the log-normal random variable X . All data was pooled together globally for computing the least squares fit to the data for each antenna combination. Therefore, the measured data from all rooms was used to calculate the model parameters of equation (4). A scatter plot of the path loss vs distance along with the least squares fit to the data is shown in Fig. 2 for each antenna combination, where the path loss is represented as a positive quantity. A cumulative distribution of the deviation between the fitted and measured data is plotted versus the normal CDF in Fig.

3, which shows that the shadow fading is log-normally distributed.

The path loss exponent for the omni/omni case is equal to 1.55, and is equal to 1.65 for the omni/dir case. The former path loss exponent is less than the latter due to the fact that an omni-directional receiving antenna collects many more multipath components in comparison to a directional receiving antenna. The path loss exponent α equals 1.72 for the dir/dir case. This value is larger than either of the latter two antenna combinations; the directional transmit antenna limits the radiated energy to a narrow cone resulting in fewer multipath components at the receiver. Note that all path loss exponents are lower than the corresponding free space value ($\alpha=2$) due to the accumulation of considerable multipath energy as opposed to a single LOS ray, which was also observed in [2][6][8]. Table 1 lists the values of the path loss exponent α and the standard deviation σ_{dB} of the shadow fading random variable X for each antenna combination.

From these results we may conclude that the path loss in the channel can be predicted as a function of distance for all three antenna combinations by using equation (4) along with the values in Table 1 and equation (1).

IV. TIME DOMAIN ANALYSIS

The impulse response of the channel was obtained by performing the IDFT on the frequency response of the channel. The frequency domain data was first filtered using a Kaiser window with $\beta=4.54$ prior to performing the IDFT. This filtering procedure reduced the side lobes of the impulse response by 50 dB and broadened the main lobe such that the time resolution has changed from 0.25 ns to 0.4 ns.

The time axis was quantized into bins to obtain a power delay profile (PDP) in which each multipath component is represented as an impulse function weighted by the integration of the power within each bin having a width $\Delta\tau=0.9768$ ns, which corresponds to a bin size slightly greater than the pulse width. Each impulse response was represented by the first arrival signal starting at time 0 s. Therefore, any multipath signal arriving within the i^{th} bin is represented by a delay $\tau_i = i\Delta\tau$, for $i=0\dots N-1$, where N is the total number of possible multipath components including the first arrival [7]. The PDP is the square of the absolute value of the discrete impulse response $h(\tau; d)$, namely $\text{PDP}=|h(\tau; d)|^2$, where $h(\tau; d)$ is represented as:

$$h(\tau; d) = \sum_{i=0}^{N-1} a_i(\tau; d) e^{j\theta_i(\tau; d)} \delta(\tau - \tau_i) \quad , \quad (5)$$

where d represents the Tx/Rx separation distance, a_i denotes the amplitude of the i^{th} multipath component, θ_i denotes the phase associated with the i^{th} multipath

component, and δ is the Dirac delta function. The noise floor was removed from the PDP prior to time quantization to eliminate noise spikes appearing as false multipath components. The noise threshold was set 2 dB above the maximum noise component detected prior to the first multipath component arrival (e.g., LOS signal). All power below this threshold was set to zero, resulting in a PDP with 98.3% energy capture after noise reduction on the average.

The multipath in the channel is most commonly characterized quantitatively by the first moment and the square root of the second central moment of the PDP, referred to as the mean delay spread and the RMS delay spread, respectively. The RMS delay spread can be used as a figure of merit for estimating data rates for multipath channels [7]. The RMS delay spread σ_τ and the mean delay spread τ_m are defined as:

$$\sigma_\tau = \sqrt{\frac{\sum_{i=0}^{N-1} (\tau_i - \tau_m)^2 |h(\tau_i; d)|^2}{\sum_{i=0}^{N-1} |h(\tau_i; d)|^2}} \quad (6)$$

$$\tau_m = \frac{\sum_{i=0}^{N-1} \tau_i \cdot |h(\tau_i; d)|^2}{\sum_{i=0}^{N-1} |h(\tau_i; d)|^2} \quad . \quad (7)$$

To obtain a stable PDP in (6) and (7), $|h(\tau; d)|^2$ is the temporal average of ten PDPs. Fig. 4 shows the CDF of σ_τ for each antenna combination. Table 2 lists the mean, minimum, median, and maximum values of σ_τ and τ_m . It is shown in Fig. 4 that the RMS delay spread decreases when directional antennas are introduced into the channel, or rather when the beamwidth of the antenna decreases. With respect to an omni-directional transmitter, the minimum RMS delay spread is decreased by 60% when using a directional receive antenna as opposed to using an omni-directional antenna at the receiver. When using a directional transmit and directional receive antenna the minimum RMS delay spread decreases by approximately 92% of the minimum RMS delay spread obtained from an omni-directional Tx/Rx antenna combination. The mean values of σ_τ for the omni/omni, omni/dir, and dir/dir Tx/Rx antenna combinations are 17.34 ns, 11.35 ns, and 7.71 ns, respectively. Results show that directional antennas used at the receiver or at both transmitter and receiver may help reduce the multipath in the channel as opposed to using omni-directional antennas. Multipath components were detected with a maximum delay up to 190 ns with respect to τ_0 for the omni/omni case and within 6 ns and 4 ns, for the

omni/dir and dir/dir antenna combinations, respectively. The average maximum excess delay for the omni/omni, omni/dir, and dir/dir antenna combinations were 143.2 ns, 121.7 ns, and 112.26 ns, respectively.

Fig. 5 shows a linear relationship between the RMS delay spread and the Tx/Rx separation distance. Although this is true for all three antenna combinations, there was a low-correlation between an increase in RMS delay spread as a function of distance when omni-directional antennas are used at the transmitter and receiver or, solely at the transmitter with a directional receiver. In contrast, there was high-correlation between an increase in RMS delay spread as a function of distance when using directional antennas at the transmitter and receiver. This trend has been observed for indoor wideband measurements [9]. RMS delay spread increased as a function of $d^{0.3}$, $d^{0.55}$, and $d^{1.01}$, for omni/omni, omni/dir, and dir/dir Tx/Rx antenna combinations, respectively. A similar result was obtained for the omni/omni antenna combination in [2], where the RMS delay spread increases as a function of distance with an exponent of 0.26.

V. CONCLUSIONS

A statistical model characterizing the path loss in the channel was developed from empirical data for three antenna pattern combinations. Statistics of the shadow fading in the environment were shown to be distributed log-normally. The RMS delay spread has been shown to decrease considerably when using directional antennas in comparison to using omni-directional antennas. Directional antennas were shown to reduce the effects of multipath in the indoor UWB channel as compared to omni-directional antennas.

This work was supported in part by the New Jersey Center for Wireless Telecommunications.

VI. REFERENCES

- [1] Federal Communications Commission, "Revision of Part 15 of the Commission's Rules Regarding Ultra-Wideband Transmission Systems. FIRST REPORT AND ORDER," *ET Docket 98-153, FCC 02-48*, pp. 1-118, Feb. 14, 2002.
- [2] S. S. Ghassemzadeh, R. Jana, C. W. Rice, W. Turin, and V. Tarokh, "A Statistical Path Loss Model For In-Home UWB Channels," in *Proc. IEEE Conf. Ultra Wideband Systems and Technol.*, pp. 59-64, May 2002.
- [3] M. Z. Win, R. A. Scholtz, and M. A. Barnes, "Ultra-Wide Bandwidth Signal Propagation for Indoor Wireless Communications," in *Proc. IEEE Int. Conf. Commun.*, pp. 56-60, June 1997.
- [4] D. Cassioli, M. Z. Win, and A. F. Molisch, "The Ultra-Wide Bandwidth Indoor Channel: From Statistical Model to Simulations," *IEEE J. Select. Areas Commun.*, vol. 20, pp. 1247-1257, Aug. 2002.
- [5] J. Keignart and N. Daniele, "Subnanosecond UWB Channel Sounding in Frequency and Temporal Domain," in *Proc. IEEE Conf. Ultra Wideband Systems and Technol.*, pp. 25-30, May 2002.
- [6] A. A. M. Saleh and R. A. Valenzuela, "A Statistical Model for Indoor Multipath Propagation," *IEEE J. Select. Areas Commun.*, vol.

SAC-5, pp. 128-137, Feb. 1987.

[7] T.S. Rappaport, *Wireless Communications: Principles and Practice*. Prentice Hall, Reprinted July 1999, Chapters 3, 4, and 5.

[8] T. S. Rappaport and D. A. Hawbaker, "Wide-Band Microwave Propagation Parameters Using Circular and Linear Polarized Antennas for Indoor Wireless Channels," *IEEE Trans. Commun.*, vol. 40, pp. 240-245, Feb. 1992.

[9] C. M. P. Ho and T. S. Rappaport, "Effects of Antenna Polarization and Beam Pattern on Multipath Delay Spread and Path Loss in Indoor Obstructed Wireless Channels," in *Proc. IEEE Int. Conf. Universal. Personal. Commun.*, pp. 04.02.1-04.02.5., 1992.

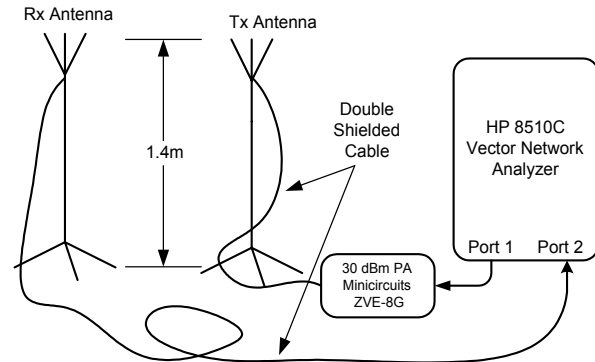


Fig. 1. Frequency domain channel sounder measurement system.

TABLE 1

Path loss exponent α and standard deviation of the shadow fading random variable X .

Antenna Combination	α	σ_{dB}
OMNI/OMNI	1.55	1.98
OMNI/DIR	1.65	1.19
DIR/DIR	1.72	0.77

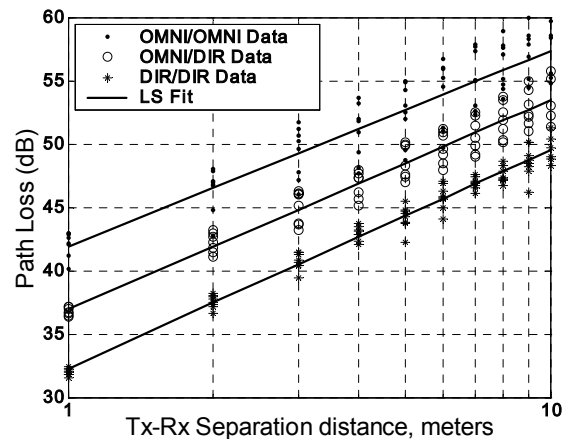


Fig. 2. Scatter plot of path loss vs. Tx/Rx separation distance.

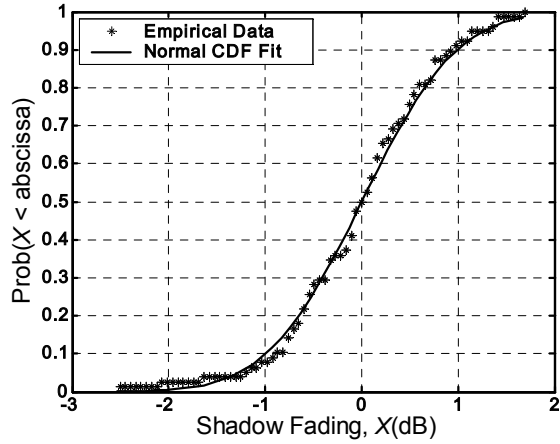


Fig. 3. CDF of shadow fading for the DIR/DIR antenna combination.

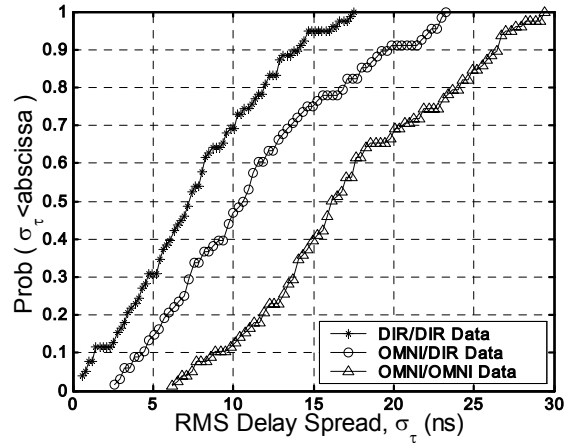
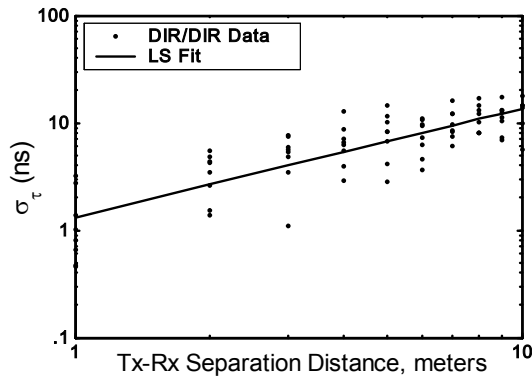


Fig. 4. CDF of RMS delay spread for each Tx/Rx antenna combination.

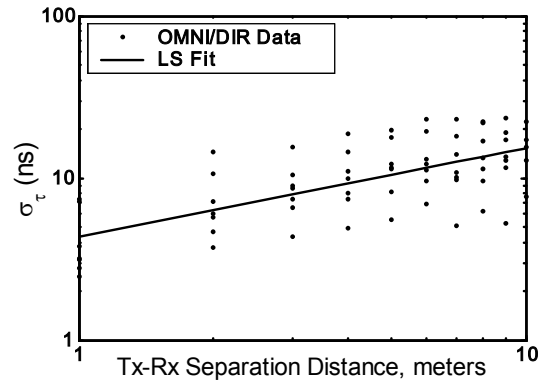
TABLE 2

Mean, minimum, median, and maximum values of σ_τ and τ_m for each antenna combination.

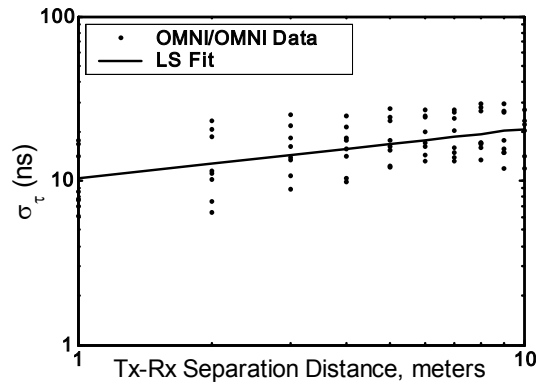
Antenna Combination	mean τ_m (ns)	min τ_m (ns)	med. τ_m (ns)	max τ_m (ns)	mean σ_τ (ns)	min σ_τ (ns)	med. σ_τ (ns)	max σ_τ (ns)
OMNI/OMNI	11.86	3.68	10.42	30.90	17.34	6.05	16.41	29.60
OMNI/DIR	5.59	0.38	4.59	16.75	11.35	2.44	10.80	23.45
DIR/DIR	2.04	0.03	1.70	7.46	7.71	0.46	7.35	17.64



(a)



(b)



(c)

Fig. 5. RMS delay spread versus distance, where (a) DIR/DIR data (b) OMNI/DIR data (c) OMNI/OMNI data.